



Plasmonic Surfaces for Cell Growth and Retrieval Triggered by Near-Infrared Light

Juan J. Giner-Casares,* Malou Henriksen-Lacey, Isabel García, and Luis M. Liz-Marzán*

Abstract: Methods for efficient detachment of cells avoiding damage are required in tissue engineering and regenerative medicine. We introduce a bottom-up approach to build plasmonic substrates using micellar block copolymer nanolithography to generate a 2D array of Au seeds, followed by chemical growth leading to anisotropic nanoparticles. The resulting plasmonic substrates show a broad plasmon band covering a wide part of the visible and near-infrared (NIR) spectral ranges. Both human and murine cells were successfully grown on the substrates. A simple functionalization step of the plasmonic substrates with the cyclic arginylglycylaspartic acid (c-RGD) peptide allowed us to tune the morphology of integrin-rich human umbilical vein endothelial cells (HUVEC). Subsequent irradiation with a NIR laser led to highly efficient detachment of the cells with cell viability confirmed using the MTT assay. We thus propose the use of such plasmonic substrates for cell growth and controlled detachment using remote near-IR irradiation, as a general method for cell culture in biomedical applications.

Controlled and non-invasive cell harvesting from responsive surfaces devoted to cell culture is of high relevance for biomedical research, regenerative medicine, and tissue engineering.^[1] The substrates should provide multivalency (be suitable for different cell types) and high biocompatibility, allowing surface biofunctionalization if needed. The cell detachment from the substrate should be minimally invasive, efficient, and ensure cell viability.^[2]

The standard procedure for detaching cells from a culture substrate includes the use of digesting enzymes which may

irreversibly damage cells, thus greatly hindering biomedical applications such as tissue engineering. Alternatively, physicochemical stimuli might induce cell detachment from substrates including electrochemical stimulus,^[3] as well as variations in pH^[4] and temperature.^[5] Fabrication of these substrates usually requires a huge synthetic effort, discarding a subsequent modification.

Remote irradiation with light stands out as one of the most convenient triggers for cell detachment. Visible green light has been used to induce cell detachment from a substrate covered with small gold nanoparticles.^[6] UV light in combination with photodegradable polymers has also been proposed to lift off cells.^[7] UV/Vis light adequately performs cell detachment, however significantly damages biological material. On the other hand, light in the near-infrared (NIR) range (800–2500 nm) appears as a highly convenient stimulus for cell detachment as it is biocompatible, displays significant transmission in biological fluids and tissues, minimal heating of aqueous media, and most importantly, no induced photo-modification of biomolecules.^[8]

Herein we introduce purpose-designed plasmonic substrates as versatile platforms for culture and retrieval of cells. The plasmonic substrates were fabricated by deposition of small Au nanoparticle “seeds”, followed by a chemical growth step leading to a dense array of branched Au nanostructures (Figure 1). This chemical route combines high plasmon efficiency and firm attachment of the nanoparticles onto the substrate.^[9] The former leads to a broad plasmon absorbance band in the red and NIR spectral regions, so that cell detachment can then be activated using NIR light. The latter provides mechanical resistance to modification by culture media and living cells.^[10]

[*] Dr. J. J. Giner-Casares, Dr. M. Henriksen-Lacey, Dr. I. García, Prof. Dr. L. M. Liz-Marzán
CIC biomaGUNE
Paseo de Miramón 182, 20009 Donostia—San Sebastián (Spain) and
Biomedical Research Networking Center in Bioengineering, Biomaterials, and Nanomedicine (CIBER-BBN)
Paseo de Miramón 182, 20009 Donostia—San Sebastián (Spain)
E-mail: jjginer@cicbiomagune.es
lizmarzan@cicbiomagune.es
Prof. Dr. L. M. Liz-Marzán
Ikerbasque, Basque Foundation for Science
48013 Bilbao (Spain)

Supporting information for this article is available on the WWW under <http://dx.doi.org/10.1002/anie.201509025>.

© 2015 The Authors. Published by Wiley-VCH Verlag GmbH & Co. KGaA. This is an open access article under the terms of the Creative Commons Attribution Non-Commercial NoDerivs License, which permits use and distribution in any medium, provided the original work is properly cited, the use is non-commercial and no modifications or adaptations are made.

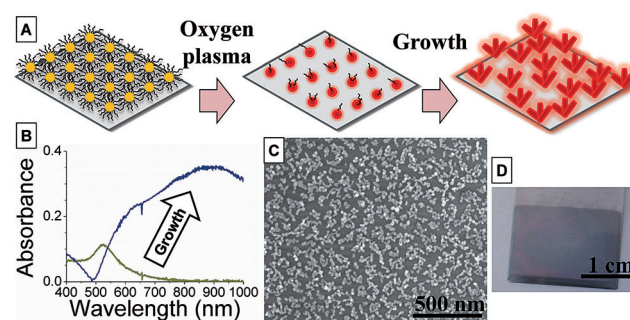


Figure 1. Fabrication of plasmonic substrates for cell culture and harvesting. A) Schematic representation of the fabrication process. B) Vis-NIR spectra of plasmonic substrates before (green line) and after (dark-blue line) the chemical growth of adsorbed Au nanoparticle seeds. C) SEM image of the plasmonic surface. D) Photograph of a plasmonic substrate on glass.

Au nanoparticles were deposited on a glass substrate by micellar block copolymer nanolithography (BCML), in which inverse micelles of the block copolymer polystyrene-*b*-poly-2-vinylpyridine (PS-*b*-P2VP) containing Au ions in the hydrophilic core, are deposited by dip-coating onto a substrate, forming a two-dimensional ordered hexagonal array.^[11] The monolayer of inverse micelles is then subjected to a short treatment of oxygen plasma for four minutes, leading to formation of Au nanoparticles with an average diameter of 15 nm. Subsequent chemical growth was induced by immersion in a solution of AuCl₄⁻ ions, ascorbic acid, and hexadecyltrimethylammonium bromide (CTAB), which yields anisotropic Au nanostructures with elongated branches pointing out in random orientations.^[12] Nanoparticles with branch lengths of about 40–60 nm and average branch diameter of about 30 nm were obtained (see Figures S1 and S2). The wide distribution of orientations of the branches and short interparticle distances (less than 10 nm) lead to extensive plasmon coupling, as shown in Figure 1.^[13] The localized surface plasmon resonance (LSPR) band shifts from a single peak centered at 525 nm, corresponding to a monolayer of small Au nanoparticles before the growth step, to a broad band ranging from 600 to 1100 nm after growth and branching. This broad plasmon band thus arises from both nanoparticle anisotropy and extensive plasmon coupling at small interparticle distances. A second treatment with oxygen plasma reduces any remaining Au ions and completely cleans the surface of the substrates by removing organic residues, as indicated by X-ray photoelectron spectroscopy (see Figure S3).^[14] This procedure can be scaled up to any desired substrate size (Figure 1D).

With the aim to promote cell adhesion we functionalized the surface of gold nanostructures with thiolated c-RGD, a cyclic three amino acid peptide that is present in many integrin-binding ligands (see structure and characterization in Figure S4). Depending on the experimental target, other thiolated biomolecules such as antibodies or DNA aptamers could also be used. Integrins constitute a transmembrane protein family forming clusters responsible for cell adhesion to surfaces, hence they are of high relevance toward tissue repair.^[15] Including the RGD biofunctional group on top of a metallic substrate by simple thiol chemistry, the morphology and intracellular signaling of integrin-expressing cells can be modified when attached.

We selected five different murine and human cell lines to test the general applicability of the plasmonic substrates for NIR-triggered detachment. We investigated the expression of the integrin α V β 3 on tumoral (HeLa and A549) and non-tumoral (HUVEC) human cells, expressing an adherent phenotype with cell spreading. We also studied the murine macrophage-like cell line J774, which whilst adherent has a more rounded phenotype but also expresses integrins which are used for a variety of roles including phagocytosis.^[16] Fluorescence microscopy (Figure 2) shows the cellular morphology on plasmonic substrates. Whereas the morphologies of HeLa, A549 and J774 cells do not vary significantly when grown on the plasmonic substrates, HUVEC cells show stretching when grown on bare (RGD-free) plasmonic

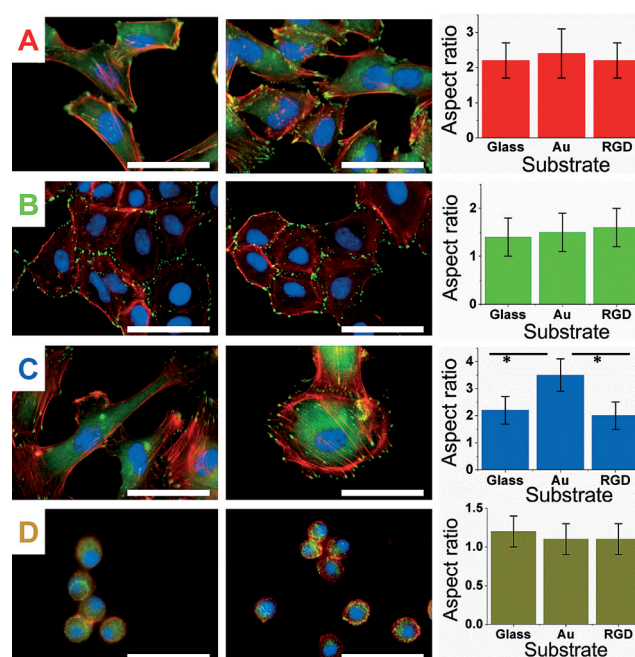


Figure 2. Study of cell morphology on plasmonic substrates as a function of integrin content in the cell membrane. A) HeLa; B) A549; C) HUVEC; D) J774. Fluorescence microscopy images of cells as grown on bare plasmonic substrates (Au, pictures on the left) and c-RGD-coated plasmonic substrates (RGD, pictures on the right). Staining was as follows: nuclei (blue), vinculin (green), actin (red). Scale bar is 50 μ m. Aspect ratio of the cells defined as the ratio between the longest and shortest dimensions. Only HUVEC cells show significant differences by Student's t-test, * $p < 0.05$.

substrates, as demonstrated by the increase in aspect ratio (Figure 2).

However, when grown on RGD-functionalized plasmonic substrates, their morphology was similar to those grown on glass (Figures S5 and S6). Changes in the morphology of the HUVEC cells by including the c-RGD peptide on the surface of the substrate can be rationalized in terms of the integrin content of these cells. HeLa and A549 cells express a low integrin content as compared to HUVEC cells, which over-express α V β 3 integrin, as determined by flow cytometry (Figure S7).^[17] HUVEC cells on bare plasmonic substrates might undergo conformational stress, as the Au nanostructures impede the regular attachment of cells on the substrates via integrin clusters. J774 macrophages show no changes in morphology which is likely due to the inherent use of integrins by macrophages as phagocytic receptors and not RGD ligand receptors.^[18] The plasmonic surfaces are therefore highly versatile, so that any biofunctional group can be incorporated using simple thiol chemistry. Control experiments were carried out with cells grown on smooth Au films as opposed to nanoparticle based films (Figures S8–S10). No significant differences in the cell growth pattern (aspect ratio, cell area or fluorescent staining to show morphology) were found, nor were cells detached upon irradiation with NIR light, indicating that the plasmonic substrates do not influence the morphology of the cells due to the nanostructure.^[19]

By exploiting the strong plasmon absorption in the NIR together with the excellent cell growth on these plasmonic substrates, successful detachment of living cells by remote NIR irradiation was realized. Functionalization with the c-RGD peptide did not influence the detachment whereas control experiments on glass slides resulted in detachment values below 10% (Figures 3 and Figures S11–S14). RGD (as

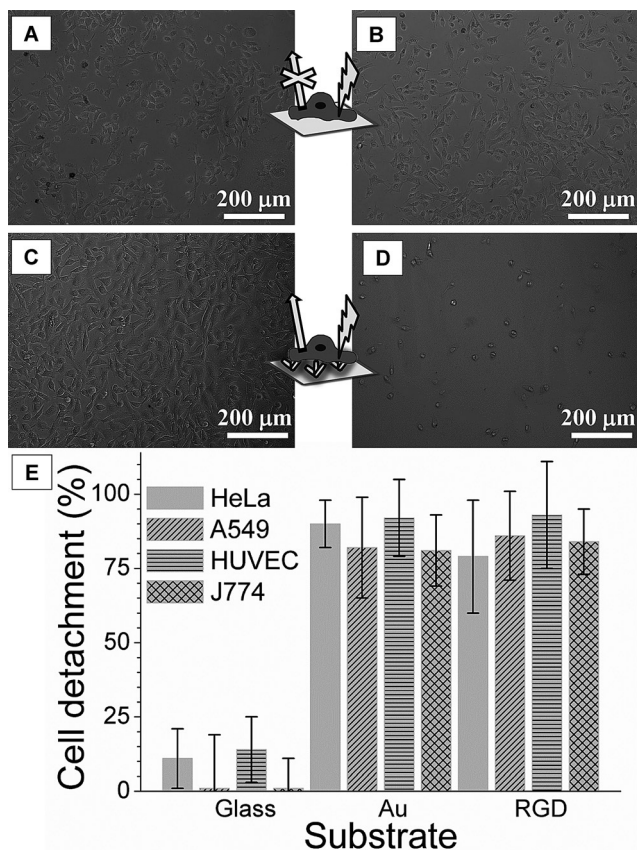


Figure 3. Cell detachment by NIR radiation. Transmitted light images of HeLa cells grown on glass (A,B) or on plasmonic substrates (C,D), before (A,C) and after (B,D) irradiation with a NIR laser at 980 nm. E) Cell detachment rates upon NIR irradiation of HeLa, A549, HUVEC and J774, as labeled. The cells were grown on glass, bare plasmonic substrates (Au), and c-RGD-coated plasmonic substrates (RGD).

most biofunctional groups) displays a size of a few nm, thus not sufficiently separating the cell from local photothermal phenomena occurring at the plasmonic surface. Each cell line required a different irradiation time and power density for detachment (Table 1). The values of power density are much lower than those in previous reports that used visible light coupled to the plasmon of individual spherical nanoparticles, usually in the range of tens of W cm^{-2} .^[20] The safety limit for the maximum power for a long exposure to skin up to 500 minutes has been set to 1 W cm^{-2} , well above the values used herein.^[21]

The detachment efficiency of cells grown on plasmonic substrates is related to the average cell area. A549 and J774 cells display the smallest area per cell (ca. 900 and $300 \mu\text{m}^2$, respectively), and were detached with an efficiency of 80%.

Table 1: Experimental conditions of NIR laser irradiation at 980 nm for cell detachment from c-RGD-coated plasmonic substrates.

Cell line	Power density [mW cm^{-2}]	Exposure time [min]	Total power [W]
HeLa	340	20	4.8
A549	340	40	4.8
HUVEC	145	5	2.0
J774	340	40	4.8
3T3 fibro-blasts	305	30	4.3

On the other hand, HeLa and HUVEC cells display a comparatively larger area per cell (1300 and $4000 \mu\text{m}^2$, respectively), and displayed detachment efficiencies approaching 100%. The irradiation time required for detachment was also shorter for HeLa and HUVEC cells than for A549 and J774 cells.

The detachment of living cells from the plasmonic substrates upon NIR irradiation may be due to a combination of phenomena at the cell-plasmonic substrate interface: photoinduced biochemical reactions, photochemical generation of reactive oxygen species (ROS), and photothermal effects. The activation of chemical reactions by NIR irradiation is unlikely, since the plasmonic substrates contain no functional groups that could be photoactivated. Additionally, NIR radiation is not typically inducing any biochemical reaction, as opposed to UV and visible light. Concerning generation of ROS, damage of the cell membrane would be expected, with subsequent cell death.^[22] On the contrary, we observe nearly complete cell survival and therefore postulate that the generation of ROS is negligible. Photothermal effects appear to be the most likely phenomenon taking place locally at the cell–substrate interface. Indeed, HUVEC cells display the largest contact area of the set of cells studied herein, and can be detached with the lowest irradiation time of only five minutes. This reduced time indicates a beneficial effect on a large contact area between cell and plasmonic substrate for the detachment. Only a mild heating of the bulk culture medium is induced by the NIR light (Figure S15), yet the increase of temperature at the nanoparticle–cell interface is expected to be higher. The localized photothermal effect is presumed to lead to the highly efficient detachment of cells, while simultaneously avoiding significant damage to cells.

The growth and detachment of 3T3 fibroblasts was also carried out. 3T3 fibroblasts produce an interconnecting extracellular matrix, commonly used as a model for tissue engineering. 3T3 fibroblasts were grown over two weeks forming a cell sheet with dimensions above $500 \mu\text{m}$ and subsequently detached using NIR laser irradiation, as described above (Figure 4). Plasmonic substrates can also be successfully applied to cell sheets, suggesting their suitability for tissue engineering.^[23]

An essential requirement for detached cells is continued viability. We confirmed cell viability using the MTT assay by transferring detached cells into a 96-well plate and allowing them to equilibrate and attach prior to performing the MTT assay (to measure metabolic activity). Cell viability seems to depend on the type of cell rather than on the experimental

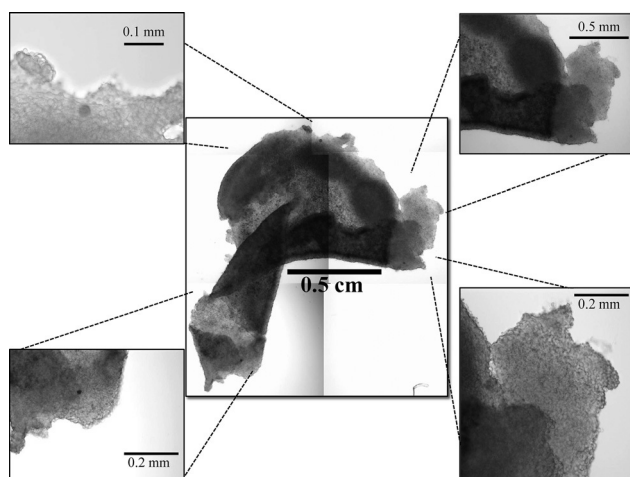


Figure 4. Detachment of a 3T3 fibroblast cell sheet. Microscopy images of a folded 3T3 NIH fibroblast sheet grown on a bare plasmonic substrate and subsequently detached by irradiation with NIR light. Detachment parameters are similar to those used for detachment of isolated cells.

conditions used for detachment such as irradiation time or power, values between 75–100% were generally obtained (Figure 5). The detached cells retain the expected morphology when re-planted on clean plasmonic substrates (Figure S16), further confirming the non-invasive nature of NIR light.

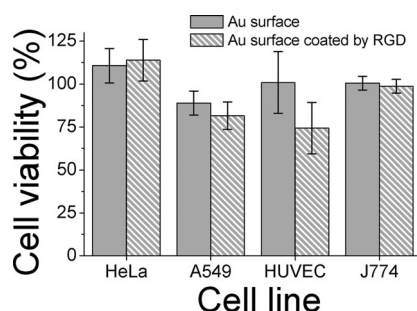


Figure 5. Cell viability, measured with the MTT assay, after NIR-mediated detachment from plasmonic substrates. HeLa, A549, HUVEC, and J774 cells were studied on both bare plasmonic substrates (solid bars) and c-RGD functionalized plasmonic substrates (columns with diagonal patterned lines).

As it is well-known that NIR laser irradiation may form small pores in the cell membrane and therefore cause cell damage,^[24] a live/dead cell assay was conducted in which live cells stain green because of the uptake of calcein-type dyes (cell membrane permeable) and dead cells stain red because of the passive uptake of propidium iodide (cell membrane non-permeable). In agreement with the MTT assay, which showed increased cytotoxicity for A549 cells after laser detachment, the live/dead assay also showed a higher proportion of dead (red) cells (Figure S17). The proportion of dead cells determined using this live/dead assay was higher in all cell lines as compared to the MTT assay. This suggests that whilst small pore formation because of laser irradiation does

occur (hence allowing the non-permeable PI dye to enter cells), this pore formation is not always cytotoxic as cells continue to have an active metabolism. The pores most likely eventually close after some time.

Reusability of the substrates was finally assessed by using a plasmonic substrate previously subjected to a cycle of cell growth and detachment. These re-used plasmonic substrates display an equivalent performance in detachment efficiency and cell viability to first-use plasmonic substrates (Figures S18 and S19).

In summary, a bottom-up approach was developed to fabricate mechanically stable nanoplasmonic substrates exhibiting extensive plasmon coupling. The substrates were used to grow a variety of cell types. Biofunctionalization with the c-RGD peptide via simple thiol chemistry could modify the morphology of integrin-rich cells. This biofunctionalization step can be performed with a variety of thiolated biomolecules, which would allow us to incorporate further recognition and responsive functionalities to the plasmonic substrates in a straightforward manner. Irradiation with a 980 nm NIR laser induced detachment of most of the cells grown on nanoplasmonic substrates, with nearly complete viability of the detached cells. The photothermal effect was identified as the main cause of cell detachment. Complete cell sheets of 3T3 fibroblasts can also be detached, showing the wide scope of this procedure not only for different cell lines but also for different forms of cell organization. Nanoplasmonic surfaces are proposed for cell culture and gentle detachment using NIR light with a huge potential in biomedicine, cell biology, and tissue engineering.

Acknowledgements

The authors acknowledge financial support from the European Research Council (ERC advanced grant number 267867 Plasmaquo). J.J. G.-C. acknowledges the Spanish Ministry of Economy and Competitiveness for a Juan de la Cierva fellowship (grant number JCI-2012-12517). A European Patent Application (EP15186375) has been presented by the authors. Dr. Luca Salassa and Emmanuel Ruggiero are gratefully acknowledged for providing access and technical assistance with the NIR laser. Dr. Luis Yate measured XPS spectra. Andrea La Porta is acknowledged for his work on graphics design.

Keywords: cell cultures · cell harvesting · gold nanoparticles · plasmonics · tissue engineering

How to cite: *Angew. Chem. Int. Ed.* **2016**, *55*, 974–978
Angew. Chem. **2016**, *128*, 986–990

- [1] a) H. S. Dhowre, S. Rajput, N. A. Russell, M. Zelzer, *Nanomedicine* **2015**, *10*, 849–871; b) A. Pulsipher, D. Dutta, W. Luo, M. N. Yousaf, *Angew. Chem. Int. Ed.* **2014**, *53*, 9487–9492; *Angew. Chem.* **2014**, *126*, 9641–9646; c) Z. Ke et al., *ACS Nano* **2015**, *9*, 62–70.
[2] Q. Zheng, S. M. Iqbal, Y. Wan, *Biotechnol. Adv.* **2013**, *31*, 1664–1675.

- [3] R. Inaba, A. Khademhosseini, H. Suzuki, J. Fukuda, *Biomaterials* **2009**, *30*, 3573–3579.
- [4] Y. H. Chen, S. H. Chang, T. J. Wang, I. J. Wang, T. H. Young, *Biomaterials* **2013**, *34*, 854–863.
- [5] Q. Yu, L. M. Johnson, G. P. López, *Adv. Funct. Mater.* **2014**, *24*, 3751–3759.
- [6] T. A. Kolesnikova, D. Kohler, A. G. Skirtach, H. Möhwald, *ACS Nano* **2012**, *6*, 9585–9595.
- [7] G. Pasparakis, T. Manouras, A. Selimis, M. Vamvakaki, P. Argitis, *Angew. Chem. Int. Ed.* **2011**, *50*, 4142–4145; *Angew. Chem.* **2011**, *123*, 4228–4231.
- [8] S. L. Jacques, *Phys. Med. Biol.* **2013**, *58*, R37–61.
- [9] J. Yuan, A. Hajebifard, C. George, P. Berini, S. Zou, *J. Colloid Interface Sci.* **2013**, *410*, 1–10.
- [10] J. A. Yang, H. T. Phan, S. Vaidya, C. J. Murphy, *Nano Lett.* **2013**, *13*, 2295–2302.
- [11] J. Matic, J. Deeg, A. Scheffold, I. Goldstein, J. P. Spatz, *Nano Lett.* **2013**, *13*, 5090–5097.
- [12] P. C. Angelomé, I. Pastoriza-Santos, J. Pérez-Juste, B. Rodríguez-González, A. Zelcer, G. J. A. A. Soler-Illia, L. M. Liz-Marzán, *Nanoscale* **2012**, *4*, 931–939.
- [13] J. J. Giner-Casares, L. M. Liz-Marzán, *Nano Today* **2014**, *9*, 365–377.
- [14] M. Arnold, E. A. Cavalcanti-Adam, R. Glass, J. Blümmel, W. Eck, M. Kantelehner, H. Kessler, J. P. Spatz, *ChemPhysChem* **2004**, *5*, 383–388.
- [15] Y. Liu, R. Medda, Z. Liu, K. Galior, K. Yehl, J. P. Spatz, E. A. Cavalcanti-Adam, K. Salaita, *Nano Lett.* **2014**, *14*, 5539–5546.
- [16] R. O. Hynes, *Cell* **1987**, *48*, 549–554.
- [17] a) Y. Zhou, Y. S. Kim, S. Chakraborty, J. Shi, H. Gao, S. Liu, *Mol. Imaging* **2011**, *10*, 386–397; b) S. L. Goodman, H. J. Grote, C. Wilm, *Biol. Open* **2012**, *1*, 329–340.
- [18] J. Savill, I. Dransfield, N. Hogg, C. Haslett, *Nature* **1990**, *343*, 170–173.
- [19] W. Chen, S. Weng, F. Zhang, S. Allen, X. Li, L. Bao, R. H. W. Lam, J. A. Macoska, S. D. Merajver, J. Fu, *ACS Nano* **2013**, *7*, 566–575.
- [20] Ž. Krpetić, P. Nativo, V. Sée, I. A. Prior, M. Brust, M. Volk, *Nano Lett.* **2010**, *10*, 4549–4554.
- [21] P. Pallavicini, S. Basile, G. Chirico, G. Dacarro, L. D'Alfonso, A. Donà, M. Patrini, A. Falqui, L. Sironi, A. Taglietti, *Chem. Commun.* **2015**, *51*, 12928–12930.
- [22] T. Labouret, J.-F. Audibert, R. B. Pansu, B. Palpant, *Small* **2015**, *11*, 4475–4479.
- [23] a) T. Kikuchi, T. Shimizu, M. Wada, M. Yamato, T. Okano, *Biomaterials* **2014**, *35*, 2428–2435; b) T. Owaki, T. Shimizu, M. Yamato, T. Okano, *Biotechnol. J.* **2014**, *9*, 904–914; c) Y. Kang, N. Mochizuki, A. Khademhosseini, J. Fukuda, Y. Yang, *Acta Biomater.* **2015**, *11*, 449–458.
- [24] R. Palankar, B. El Pinchasik, B. N. Khlebtsov, T. A. Kolesnikova, H. Möhwald, M. Winterhalter, A. G. Skirtach, *Nano Lett.* **2014**, *14*, 4273–4279.

Received: September 26, 2015

Revised: October 31, 2015

Published online: November 23, 2015